A&A manuscript no.
(will be inserted by hand later)

Your thesaurus codes are:
02.01.2; 08.02.2; 08.09.1 CAL 87; 13.25.5

ASTRONOMY
AND
ASTROPHYSICS
18.3.1996

Visual Light from the Eclipsing Supersoft X-Ray Source CAL 87

S. Schandl*, **E. Meyer-Hofmeister, F. Meyer**

Max-Planck-Institut für Astrophysik, Karl Schwarzschildstr. 1, 85740 Garching, Germany

Received date; accepted date

Abstract. We calculate the visual light curve of CAL 87 based on the assumption that an accreting steadily burning white dwarf irradiates the accretion disk and the secondary star, as suggested by van den Heuvel et al. (1992). We find a reasonable fit including the following sources of visual light: 1. the secondary star where the energy from irradiation is spread out over the surface, 2. the accretion disk with an optically thick, cold, clumpy spray presumably caused by an accretion stream of high mass flow rate impinging on the disk (hot spot). This spray moving around the disk can account for the asymmetry in the light curve and the depth of the secondary minimum. This supports the assumption that the white dwarf is permanently hidden by the disk.

Key words: accretion disks – binaries: eclipsing – stars: CAL 87 – X-rays: stars

1. Introduction

Luminous X–ray sources with very soft spectra had already been found with the IPC detector of the EINSTEIN X–ray observatory. The ROSAT observations now led to the discovery of many new sources of this kind, and a separate class, the supersoft sources (SSS), has been established. The SSS are luminous X–ray objects with very soft spectra (more than 90% of the observed photons below 0.5 keV). This corresponds to a blackbody temperature of $10^5 - 10^6$ K. The bolometric luminosity is close to the Eddington limit which for a 1M$_\odot$ star is $L_{\rm x} \simeq 10^{38}$ erg/s. Up to now about 25 to 30 objects have been found in our galaxy, in the Magellanic Clouds and the Andromeda Nebula.

Such luminosities and temperatures correspond to blackbody surfaces of typical white dwarf dimension, $r \simeq 10^9$ cm. The very soft spectra can originate from different kinds of objects where we might expect a hot and possibly accreting white dwarf as in novae, planetary nebulae, symbiotic binaries but possibly even from neutron stars surrounded by an appropriate cocoon of gas (for recent reviews see Hasinger (1994), Kahabka et al. (1994)). From the different behaviour of the observed SSS (variability, on– and off–states) one might conclude that they do not form one unique class of objects.

Optical counterparts of several SSS were found, mainly blue objects. It was argued that the irradiated accretion disk around the compact object would be the dominant optical light source (van den Heuvel et al. 1992, later referred to as vdH). For several systems orbital periods are known: e.g. CAL 83 (25 hr, Smale et al. 1988), CAL 87 (10.6 hr, Callanan et al. 1989) and RX J0019 (15.8 hr, Beuermann et al. 1995). The periods give constraints on the geometry of the binary system. Especially for CAL 87 important information comes from the optical and X-ray eclipse light curves (Cowley et al. 1990, Schmidtke et al. 1993, Kahabka et al. 1994).

In an earlier attempt to model the optical light curve Callanan & Charles (1989) used a numerical code of Hellier & Mason (1989) for a simulation of CAL 87 as a LMXB. They already found an elevated disk rim as useful for such a simulation.

The aim of our present investigations is to determine a theoretical light curve for CAL 87, based on the model of vdH for steady nuclear burning on accreting white dwarfs. We model the contributions from the accretion disk, hot spot spray and the secondary star, each of them illuminated by the central hot white dwarf. Following the results of vdH we have a narrow range of possible mass accretion rates, white dwarf masses and secondary star masses. We obtained values listed in Tab. 1. Additionally, as shown later, the well observed optical light curve puts severe constraints on the theoretical model.

In section 2 we discuss the observed light curve, especially the asymmetry in the ingress and egress of the primary minimum in connection with the interaction between the accretion stream and the disk. This lets us consider a cold clumpy spray which is illuminated by the white dwarf and whose brightness varies for the observer with orbital period. We compare this feature with the signature of the interaction of accretion stream and disk in light curves of eclipsing nova-like cataclysmic variables.

In section 3 we describe how we model the visual radiation from secondary star, accretion disk and spray. We take the source of illumination, the white dwarf, as a point source. The radiation from the secondary star is evaluated as resulting from surface elements on the equipotential surface of a Roche lobe filling star. The disk height is determined consistently with the

* email: suh@mpa-garching.mpg.de

Table 1. The System Parameters

Observations:			
orbital period [1]	P	=	10.6 h
distance to LMC	d	=	57.5 kpc
SSS-model dependent parameters [2]:			
white dwarf	M_1	=	0.75 $M_\odot$
secondary star	M_2	=	1.5 $M_\odot$
mass accretion rate	$\dot{M}$	=	$0.8\,10^{-7}$ $M_\odot$/yr
=> separation	a	=	$2.2\,10^{11}$ cm
=> luminosity of WD	L	=	$2.2\,10^{37}$ erg/sec
Parameters used in the simulation:			
temperature of the non-irr. sec. star [3]	$T_\star$	=	8000 K
efficiency of radiation reprocessing	η	=	0.5
inclination	i	=	77°

References: 1 Callanan et al. (1989), 2 van den Heuvel et al. (1992), 3 Schaller et al. (1992)

irradiation. The efficiency of reprocessing to thermal radiation is taken as a parameter. We used an angle resolution of 1° for the surface elements of the star and 200 concentric rings and also 1° resolution in azimuth for the disk. For the shape of the spray we included information from ballistic trajectories.

In section 4 we present the results of our modelling. Comparing with the observed light curve we find that it is necessary to include both, essential energy transport from the bright side of the secondary to non-illuminated parts and a large volume of the spray. We show four models to explain the different effects: model a (simple), b (including the spray), c (with energy transport to un-illuminated parts of the secondary) and d (with modifications of model b and c together).

The discussion in section 5 summarizes what we can learn from modelling the observed light curve for the SSS CAL 87. Studying how this system would appear if we would see it under different inclinations, we find that these other light curves are quite similar to the light curves of CAL 83 and RX J0019.

2. Observational and theoretical constraints

Looking to the light curve of CAL 87 its asymmetry will be noticed immediately. In this paper we want to follow the idea that the interaction of the accretion stream with the disk rim could be the origin of this: Looking to the basic constituents of a binary system, the compact star, its companion, the disk and the mass flow, only the effects of the hot spot can add an asymmetric component to the light curve. The high accretion rate suggested in the vdH model on the order of $10^{-7}\,M_\odot/\mathrm{yr}$ could lead to rather dramatic effects when this gas impinges the disk rim. In other X-ray binaries such sprays have already been considered.

The asymmetry of the light curves of eclipsing nova-like cataclysmic variables is also understood as resulting from the hot spot (e.g. Smak 1971, Smak 1994). In these systems the companion does not significantly contribute to the optical light and one observes only the disk and the hot spot. Their maximal optical light is observed just before the eclipse of the disk when we look directly towards the hot spot which is then located in front of the white dwarf (see Fig. 1 for the geometry which is the same for all close binaries with mass transfer). – In contrast, CAL 87 shows more optical luminosity *after* eclipse than before. In the model this is a natural consequence of the hot spot and the irradiation effect: The geometrical thick hot spot region acts as a large screen collecting a lot of radiation flux of the white dwarf. The emitted reprocessed optical light can be well observed at orbital phases where the hot spot is behind the white dwarf, that is after the eclipse (Fig. 1). Before eclipse we look against the non-irradiated outer rim of this area which covers the illuminated inner disk regions (Callanan et al. 1989, Cowley et al. 1990).

The optical light curve of LMXB 4U 1822-37 shown by Mason et al. (1980) is similar to that of CAL 87. Also there the intensity drop at the phases before eclipse was connected to the interaction between accretion stream and disk. Hellier & Mason (1989) modelled the optical and X-ray light curves including a bulge around phase 0.8 or two bulges around phase 0.8 and 0.2 where they connect the 0.8 – bulge with the impact of the accretion stream on the disk (where their phase 0.8 corresponds to 72° in our notation, see e.g. Fig. 2 below). In their simulation they added normalization parameters for the emission of the disk rim and the inner disk and also took for the illuminated secondary an optional constant plus sinusoidal component.

Noting this similarity Callanan & Charles (1989) calculated a fit to the light curve of CAL 87 using a similar model to that used in determining the disk structure of LMXB 4U 1822-37 by Hellier & Mason (1989). The stellar masses in their LMXB model for CAL 87 are presumably different from those expected now (mass ratio $q \simeq 0.2$ in Hellier & Mason (1989), q = 2 here). The phase dependence of the secondary's light described as a constant plus sinusoidal seems not to be adequate (compare the light curve in our Figure 3, model a and b).

For our analysis we first developed models for the hot spot region with a small vertical extension, without success. The total luminosity and the shape of the light curve (secondary minimum) did not nearly fit the observations. Instead of this, models with a thick structure at the disk rim allow to find a proper fit with small variations of the involved quantities

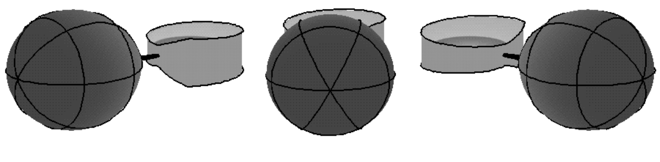

Fig. 1. A model of CAL 87 around eclipse.

(radius, height and temperature) in agreement with a similar result by Hellier and Mason (1980) for their simulations before.

This description is also supported by the low L_x/L_{opt} ratio suggesting that the central X-ray source is hidden from direct view similar to LMXBs, as supposed by Pakull et al. (1988). Additionally, there would be a deep eclipse in the X-ray light curve if the observed X-rays originated from the central white dwarf and not from scattering of surrounding gas as the observations suggest (Schmidtke et al. 1993, Kahabka et al. 1994). In order to cover the source the optically thick region has to have a vertical extension at each angle of azimuth of $z/r \geq (\pi/2 - inclination)$ which is about 0.25 in our calculations. The maximal simulated opening angle of the gas will be 0.45.

We compare this to the scale height of the disk $H_{\rm disk}/r = 0.04\,T_4^{1/2}$ and of an X-ray induced corona $H_{\rm cor}/r = 0.25\,T_{5.6}^{1/2}$ where the temperature $T = 10^{5.6}$ K corresponds to the X-ray flux obtained by the vdH model. Therefore, cold matter can not reach the required vertical height in form of a hydrostatic layering. Although the coronal scale height is of the right order it will not be optically thick to cover the central source continuously.

Therefore, the observed optical light has to be emitted by a cold and clumpy gas. This spray is embedded in the hot corona and both are in pressure equilibrium. All spray matter should then cover the central white dwarf all the time. Expelled in all directions the spray must move along free fall trajectories around the accretion disk. This can explain the large vertical height required to reproduce the observations mentioned above.

Although the hydrodynamic generation of such a two phase medium is not yet fully understood there are several conclusive arguments for their existence. Howarth & Wilson (1983) and Karitskaya et al. (1986) observed cold blobs ($T \simeq 10^{4.4}$ K) with number densities of $n \simeq 10^{13.3}$ cm^{-3} of the X-ray binary HZ Her/Her X-1 in optical and UV data. Bochkarev & Karitskaya (1989) suggested a physical model for these observed blobs. Schandl (1996) showed that the spray generated by a stream impinging onto a warped disk surface generates the preeclipse dips in the X-ray light curve of Her X-1. Frank et al. (1987) explained with such a two phase medium the optical light curves of dipping and coronal LMXBs. Also the observations of Cal 87 (Hutchings et al. 1995) showing gas in the temperature range between 25000 K and 29000 K around eclipse are consistent with such a spray.

Summarizing, the asymmetry in the optical light curve, the depth of the secondary minimum, the low L_x/L_{opt} ratio and the small decrease in X-rays during the deep optical eclipse may be understood by an optically thick spray of large vertical height which permanently covers the white dwarf.

3. The simulation

3.1. The secondary star

We describe the surface of the secondary star with a spherical grid of 1° resolution in the polar and the azimuthal angles. Further on, the grid points lie on the equipotential surface of the Roche lobe of the star.

The observation of the secondary star is difficult because of a star which is in the close projected vicinity of CAL 87. After subtracting the light of this star the remaining spectrum shows apparently no signature of the secondary star (Pakull et al. 1988 and private communication 1995). Therefore we assume a temperature for the non-irradiated secondary of about $T_\star = 8000$ K as calculated for a main sequence star of 1.5 $M_\odot$ with a radius of 9.7 10^{10} cm (= Roche radius) and 0.25 solar metallicity specific for the LMC (Schaller et al. 1992).

We describe the source of radiation, the white dwarf, as a point source. The irradiation of each surface element of the secondary depends on the angle of incidence θ and one obtains for the temperature of the irradiated star

$$\sigma T_{\star \rm irr}^4 = \sigma T_\star^4 + \eta \, \frac{L}{4\pi\, r^2} \, \cos\theta \qquad (1)$$

with σ Stefan-Boltzmann constant, r distance between the white dwarf and the surface element. The parameter η is the efficiency of the reprocessing of the illuminating radiation from the white dwarf to thermal radiation, comparable to $(1 - a)$ where a is the albedo.

Depending on the geometry there is no irradiation of surface areas located behind the illumination horizon or in the shadow of the accretion disk (see Fig. 3 model a or b).

In some models below we include energy transport from irradiated to non-irradiated parts of the stellar surface. We took a simple description because the correct solution of this problem is complex and beyond the scope of this paper. We spread the luminosity $\sigma T_{\star \rm irr}^4 \, dq$ of each surface element with area dq weighted by a Gaussian kernel and integrate over the whole surface. The resulting luminosity of each surface element is

$$\sigma T_{\star \rm irr,spread}^4 \, dq = \mathcal{N} \, dq \int \sigma T_{\star,\rm irr}^{\prime 4} \, \exp\left(-\beta'^2/B^2\right) dq'. \qquad (2)$$

β is the angle between the normal vectors of the surface elements dq and dq' and the parameter B describes the angular width of the spreading. In our simulations we use $B = 45°$. The normalization constant $\mathcal{N}$ achieves the equality of the total luminosity of the star with and without energy transport:

$$\int \sigma T_{\star \rm irr,spread}^4 \, dq = \int \sigma T_{\star \rm irr}^4 \, dq. \qquad (3)$$

We take a black body spectrum for the emitted radiation of the secondary star where λ is the wavelength, h the Planck constant, c velocity of light and k the Boltzmann constant,

$$B_\lambda(T) = \frac{2\,h\,c^2}{\lambda^5} \, \frac{1}{\exp\left(\frac{hc}{kT\lambda}\right) - 1}. \qquad (4)$$

This radiation flux is folded with an optical filter function $w(\lambda)$ (Allen 1973) to get the optical flux of each surface element

$$f_{\rm opt} = \int_{\rm filter} \pi \, B_\lambda(T) \; w(\lambda) \; d\lambda. \qquad (5)$$

Finally the total observed optical flux is calculated using the angle ϑ between the normal vector of the surface element and the direction to earth:

$$F_{\star\mathrm{total,opt}} = \frac{1}{\pi d^2} \int f_{\mathrm{opt}} \cos\vartheta \, dq \tag{6}$$

3.2. The accretion disk

This section describes the disk without any interaction with the accretion stream. The modifications due to the spray are the topic of the next section.

The disk height z_0 (height of the photosphere above midplane) of the irradiated disk was determined from vertical structure computations for several values of $\dot{M}$, M_1 and α consistently. Approximation by power law gives

$$z_0/r = 10^{-0.95}\, r_{11}^{0.093} \left(\frac{M_1}{\mathrm{M}_\odot}\right)^{-0.38} \dot{M}_{-7}^{0.17}\, \alpha_{0.3}^{-0.12}. \tag{7}$$

The disk temperature is determined by frictional heating and irradiation, with θ again angle of incidence

$$\sigma T_{\mathrm{d,irr}}^4 = \frac{3}{8\pi}\frac{G M_1 \dot{M}}{r^3} + \eta \frac{L}{4\pi r^2} \cos\theta \tag{8}$$

with G the constant of gravitation. The visual light of the black body radiation is calculated following Eqs. (4) - (6).

The disk size is taken as $r_{\mathrm{d}} = 0.8\, r_{\mathrm{L}}$ (r_{L} Roche lobe radius) according to the models of Paczyński (1977) and Papaloizou & Pringle (1977).

3.3. The spray

We model the optically thick surface of the spray matter in form of an increase of the disk size, height and temperature. As observed by Hutchings et al. (1995) the temperature around eclipse is between 25000 K and 29000 K. Due to the illumination by the white dwarf, the corresponding surface temperature increases (see Eq. 8) and increases the observed mean temperature of all surface elements. We assume the lower observed limit, 25000 K, for the temperature of the un-illuminated spray.

The spray moves not only along the disk rim but also towards smaller disk radii ($r < 0.8\, r_{\mathrm{L}}$). But during our investigations we found that there is no real difference in the final light curve between solutions which also modify temperature and height at these inner disk regions. The reason is the high inclination of CAL 87 which makes the vertical extension much more relevant than the radial one. Therefore we restrict the modification of the disk shape to radii $r \geq 0.8\, r_{\mathrm{L}}$.

In Fig. 2 the radial and vertical modifications are shown in dependence on the azimuth ϕ starting at the phase of impact. The radius increases up to $r = 1.2\, r_{\mathrm{L}}$ at about $\phi = 45°$ and decreases at later phases to its original value. This model follows calculations of free fall trajectories of matter expelled at the hot spot. The maximal vertical extension of the disk of about $z/r = 0.45$ and the maximal radial extension are placed at about 45° after the impact.

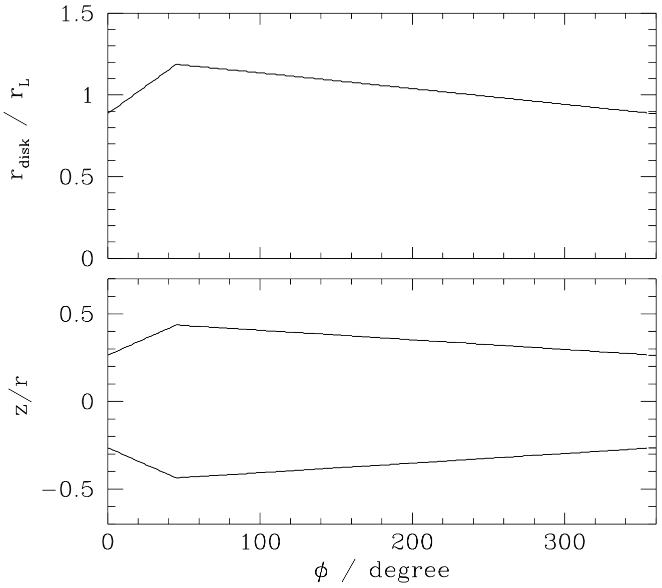

Fig. 2. The upper panel shows the disk radius dependent on the azimuth where $\phi = 0$ is the phase of impact. The maximal disk height z/r of the hot spot is represented in the lower diagram.

The irradiation of the spray is calculated according to Eq. (1), the spectrum is taken as black body and the final optical flux calculation is performed in the same way as for the secondary star.

Numerically we describe the disk modified by the spray in polar coordinates with a resolution of 1° in azimuth using 200 concentric rings. Because the disk size varies with the azimuth some outer surface elements do not contribute.

4. The effect of spray and energy transport on the light curve

Figure 3 shows four different models with and without the effects of the spray and the energy transport (see table 2). For comparison we set the inclination of all models equal to 77° as this is the best value for our final fit model d. The efficiency parameter $\eta = 0.5$ is changed only for model b to $\eta = 1$ to reproduce the total luminosity.

Table 2. The differences between the models

model	spray	energy transport	η
a	no	no	0.5
b	yes	no	1.0
c	no	yes	0.5
d	yes	yes	0.5

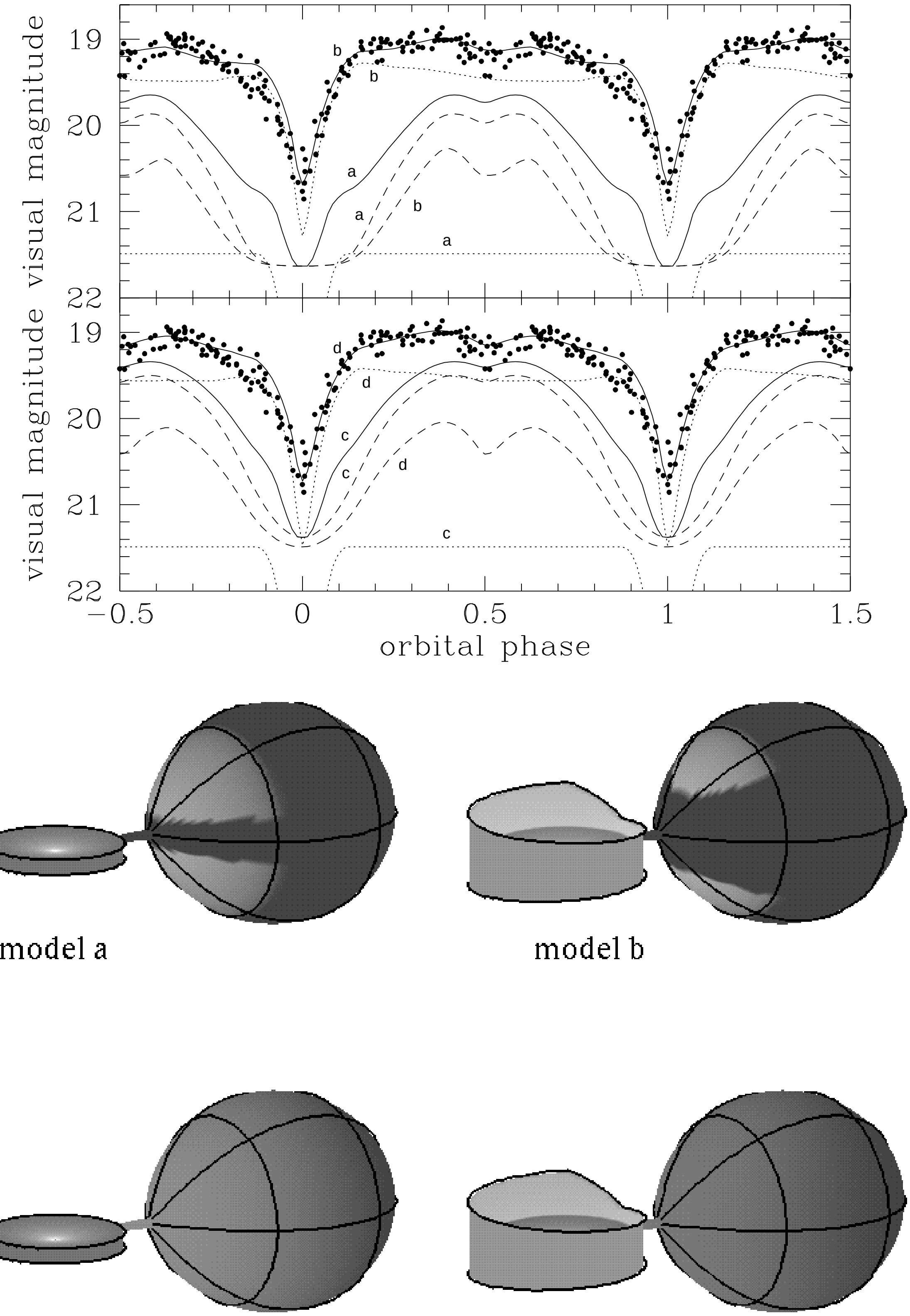

Fig. 3. Shown are light curves of four simulations corresponding to model a and b (upper panel), c and d (lower panel). For a detailed description see section 4. For each model the simulated optical light curve (solid lines) and the contribution of the star (dashed lines) and the disk (dotted lines) are drawn. The dots show the composite V light curve of CAL 87. The photometry is done between 1985 November and 1992 December (Schmidtke et al. 1993). A view to the systems at $\phi_{\rm orbit} = 0.35$ is shown below (1/4 resolution of the calculations).

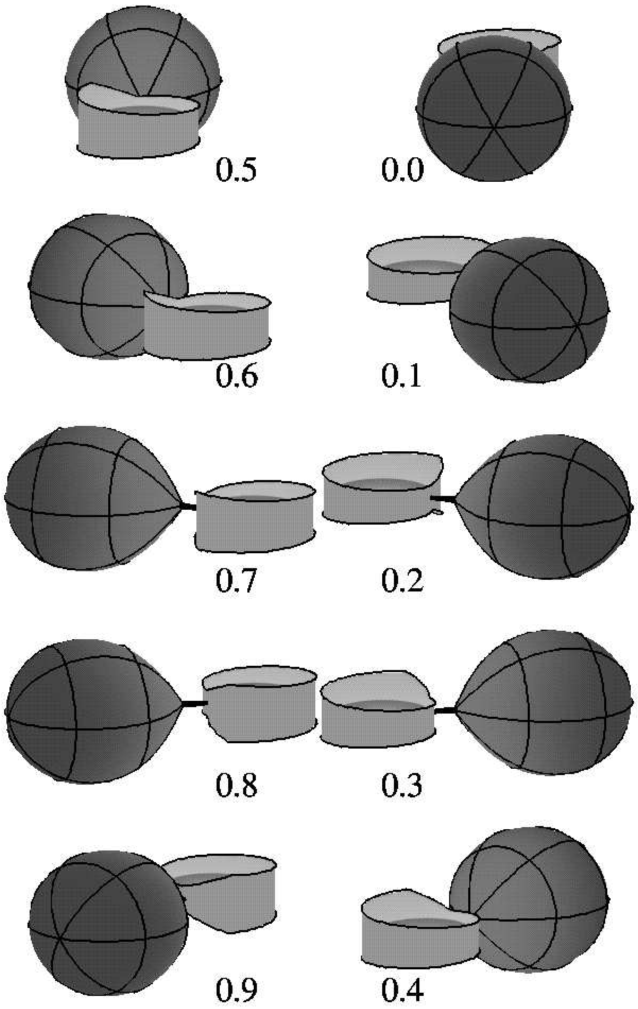

Fig. 4. This figure illustrates an orbit of the system (model d) at ten different phases. Left column $\phi = 0.5-0.9$, right column $\phi = 0.0-0.4$.

4.1. Model a

Model a consists of a disk not modified by the spray and a star without energy transport. This solution shows that the contribution of the disk itself is too small to reproduce the high luminosity around eclipse. At these phases ($\phi = 0.9 - 1.1$) the non-illuminated surface of the star shows only a constant signal. In contrast to this the width of the simulated eclipse fits the data very well. In connection with the V-shaped eclipse, this indicates an extension of the eclipsed body comparable to the disk size. a hot spot located only in the vicinity of the impact would produce a narrower U-shaped eclipse like that of a point source. Thus the effect of the stream–disk interaction has to modify the whole disk rim as the spray might do.

Because of the thin disk, the shadow on the secondary is small. The resulting large irradiated area yields a high luminosity around $\phi = 0.5$ where we look directly to the bright front side. Due to the small projected area of a thin disk also the depth of the secondary minimum around $\phi = 0.5$ is weak. This disk barely covers the secondary.

4.2. Model b

In contrast, the disk together with the spray produces a deeper secondary minimum shown in model b (see Fig. 4 for illustration of the different orbital phases). Its irradiated area is smaller than in model a and the overall contribution of the star is less although we set the efficiency parameter $\eta = 1$.

This model of a spray at the disk rim reproduces the observed data much better compared to model a. Only the width of the eclipse is too small although most optical light comes from the spray at the outer disk regions. This indicates that the disk is even larger or that the secondary contributes to the luminosity at these phases ($\phi = 0.0 \pm 0.1$). For the latter possibility we now investigate the effect of a transport of energy on the secondary.

4.3. Model c

We set the energy transport width $B = 45°$ in Eq. (2). This value also fits the averaged blue light curve of the X-ray binary Her X-1 which is a binary with an irradiated 2.2 $M_\odot$ companion suggesting a comparable stellar structure as in CAL 87. The advantage of that system is that there the contribution of the accretion disk to the optical light curve is small because of its special geometrical structure and thus nearly the whole light can be assigned to the secondary.

In general we find, the larger the transport width B, the larger the range of suitable fits. Model c corresponds to model a, but energy transport of width 45° is included. Even at phase $\phi = 0.0$ the star is brighter due to energy transported to the back side of the star. Due to this the width of the minimum of the stellar contribution is smaller when compared to models a and b. The clear increase of the optical stellar light between phases $\phi = 0.0$ and $\phi = 0.1$ reduces the demands on the disk luminosity.

The stellar luminosity is larger than in model a even around $\phi = 0.5$ where we look directly to the irradiated stellar surface. The directly illuminated parts contribute less than in model a, but the heated regions in the shadow and behind the illumination horizon contribute more than before, especially because of the lower bolometric corrections for these lower temperatures (Eq. (5)).

This shift of energy into the wavelength range of the optical filter is even more evident in the comparison of the stars of model b and d, although η of model b is twice that of model d.

4.4. Model d

Model d includes energy transport on the secondary and the spray described in section 3.3. It combines two striking features of the light curve: (1) the strong depth of the secondary minimum is obtained by the spray because its large projected area covers the secondary well, (2) a slightly better fit around eclipse compared to model b results from the energy transport on the secondary, which contributes to the light curve at these phases, reducing the strong demand on the disk. Additionally, because of the more realistic efficiency parameter $\eta = 0.5$ we prefer model d to model b.

The solution agrees with the predictions of Cowley et al. (1990) who suggest that there is no significant heating of the secondary. vdH described the heated side of the star to be at least three times brighter than the non-heated side. This is also reproduced in model d.

5. Discussion

5.1. The extended spray region at the disk rim

As a consequence of the extended spray model the white dwarf is never directly observable. This is supported by the observation of a rather low X-ray luminosity $L_x \simeq 10^{36} - \simeq 10^{37}$ erg/sec (Pakull et al. 1988, Greiner 1995, private communication) compared to other known X-ray binaries with luminosities on the order of $L_x \simeq 10^{38}$ erg/sec.

Simulations of relatively thin hot spot regions which allow a view to the white dwarf at each phase did not fit the data. Their luminosity is to small by two magnitudes. Additionally, the direct view to the white dwarf described as a point source would result in a deep and wide eclipse which would last about 0.12 in orbital phase. Another problem with thin disks is the depth of the secondary minimum which is caused by the disk covering a part of the star (see models a and c). An extended spray, on the other hand, generates the observed depth.

An interesting point to note is the scattering of the data of Schmidtke et al. (1993). Apparently it is less during the eclipse, but this is misleading: Subtracting a mean light curve one obtains a constant amplitude of the deviations, even during eclipse, see Fig. 5. Therefore, the scattering is produced in a region larger than the disk/star system. Because of the observed P Cygni profiles in some systems a wind is a promising candidate for the scattering medium. This would also explain the less deep X-ray eclipse.

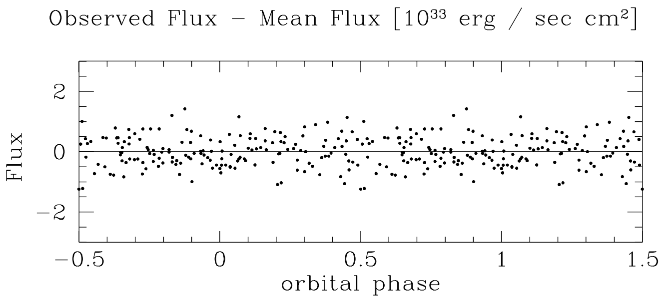

Fig. 5. The observed data (Schmidtke et al. 1993) minus the mean light curve. The scattering does not depend on the orbital phase suggesting a scattering region much larger than the disk size.

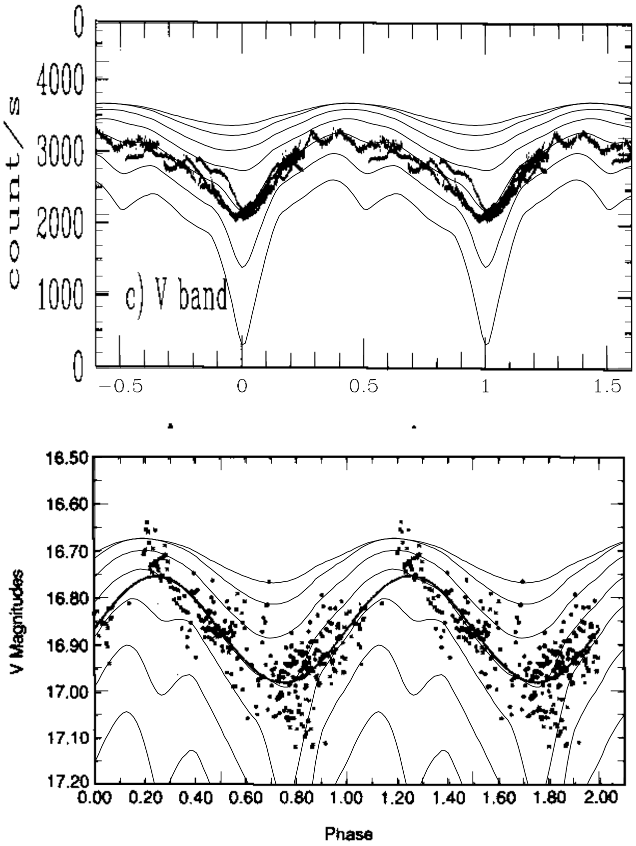

Fig. 6. The light curves of CAL 87, model d, if the system would be seen under different inclinations. Both diagrams show solutions for inclinations 20° (top) to 80° (bottom) in steps of 10°. Additionally we scanned the light curves of RX J0019 (upper panel, from Beuermann et al. 1995) and CAL 83 (lower panel, from Smale et al. 1988).

5.2. Comparison to other supersoft sources

There are at least two other supersoft sources with well observed optical light curves, Cal 83 (Smale et al. 1988) and RX J0019 (Beuermann et al. 1995). Both light curves show no eclipse indicating a lower inclination than that of CAL 87. This raises the question how the light curve of CAL 87 would appear if we saw the system under other inclinations. We show these light curves in Fig. 6 and superimposed the observations of Cal 83 (Smale et al. 1988) and RX J0019 (Beuermann et al. 1995). We find good agreement between the simulation of CAL 87 seen under $i \simeq 50°$ and Cal 83, and also between the simulation $i \simeq 60°$ and RX J0019. The latter is quite different from the value $i \simeq 20°$ estimated by Beuermann et al. (1995) from Doppler shifts of HeII lines in the case that they originate near the white dwarf. Simulating different inclinations of model b shows, that in the case of no energy transport the inclination should be even a bit higher to reproduce the observed orbital light variation.

The surprisingly good agreement suggests common main features in SSSs. This supports models where the spray dominates the optical light curves, because the unusually high accretion rate resulting in a strong interaction of stream and disk rim is common to all of them. We have not computed light curves for other system parameters as higher masses or larger disks. The periods of the binary seem to play a minor role in this context. This is not surprising if we keep in mind, that the geometry of CAL 87 depends only on the mass ratio of the binary stars and that the possible mass ratios according to the vdH model lie in a narrow range.

6. Conclusions

Following the model of vdH we find a reasonable fit for the visual light curve of CAL 87 including the secondary, the disk and an extended spray region. This extended region presumably created by the material impinging on the disk acts like a screen for the radiation from the hot white dwarf and provides the high amount of optical light, which cannot originate in a thin disk (Meyer & Meyer-Hofmeister 1995). This results in a permanently hidden white dwarf, covered by the spray, supported by the low observed X-ray luminosity on the order of 1–10% of other LMXBs and supersoft sources, (Pakull et al. 1988, Greiner 1995, private communication). We found that thin hot spot descriptions resulting in a direct view toward the white dwarf were not successful.

Including energy transport of the irradiated flux to non-illuminated parts on the secondary surface yields slightly better results around primary eclipse. It increases the visual light from the secondary because of lower bolometric corrections. Therefore, one obtains a high stellar contribution to the light curve using a reasonable efficiency parameter of radiation reprocessing, even if the irradiated surface area is small because of the large disk shadow.

Acknowledgements. We are grateful to Paul Schmidtke who kindly provided original data of CAL 87. We thank Jochen Greiner, Peter Kahabka and Hans–Christoph Thomas for information and many interesting discussions and the anonymous referee for calling our attention to the paper of Callanan and Charles (1989).

References

Allen C.W., 1973, Astrophysical Quantities, 3rd edition, Univ. London, The Athlone Press, p.205
Beuermann K., Reinsch K., Barwig H. et al., 1995, A&A 294, L1
Bochkarev, N.G., Karitskaya, E.A., 1989, Ap&SS 154, 189
Callanan P.J., Charles P.A., 1989, ESA SP-296, 23rd ESLAB symposium, p139
Callanan P.J., Machin G., Naylor T., Charles P.A., 1989, MNRAS 241, 37
Cowley A.P., Schmidtke P.C., Crampton D., Hutchings J.B., 1990, ApJ 350, 288
Frank J., King A.R., Lasota J.-P., 1987, A&A 178, 137
Hasinger G., 1994, Reviews in Modern Astronomy 7, p129, ed G. Klare, Astron. Gesellschaft
Hellier C., Mason K.O., 1989, MNRAS 239, 715
Howarth, I.D., Wilson, B., 1983, MNRAS 204, 1091
Hutchings J.B., Cowley A.P., Schmidtke P.C., Crampton D., 1995, AJ 110, 2394
Kahabka P., Pietsch W., Hasinger G., 1994, A&A, 288, 538
Karitskaya E.A., Bochkarev N.G., Gnedin Y.N., 1986, Astron. Zh. 63, 1001
Mason K.O., Middleditch J., Nelson J.E., et al., 1980, ApJ 242, L109
Meyer F., Meyer-Hofmeister E., 1995, Cataclysmic Variables, A. Bianchini et al. (eds.), Kluwer Academic Publishers, p. 463
Paczyński B.,1977, ApJ 216, 822
Pakull M.W., Beuermann K., van der Klis M., von Paradijs J., 1988, A&A 203, L27
Papaloizou J., Pringle J.E., 1977, MNRAS 181, 441
Schaller G., Schaerer D., Meynet G., Maeder A., 1992, A&AS 96, 269
Schandl S., 1996, A&A in press
Schmidtke P.C., McGrath T.K., Cowley A.P., Frattare L.M., 1993, PASP 105, 863
Smak J., 1971, Acta astr. 21, 15
Smak J., 1994, Acta astr. 44, 59
Smale A.P., Corbet R.H.D., Charles P.A. et al., 1988, MNRAS 233, 51
van den Heuvel E.P.J., Bhattacharya D., Nomoto K., Rappaport S.A., 1992, A&A, 262, 97 (vdH)

This article was processed by the author using Springer-Verlag LaTeX A&A style file *L-AA* version 3.